Bull. Chem. Soc. Jpn., 72, 661—667 (1999)


# A Study of Electron Spin Polarization Transfer in a System of Photo-Excited Triplet Phthalocyanine and a Nitroxide Radical

**Islam SM Saiful, Jun-ichi Fujisawa, Nagao Kobayashi,† Yasunori Ohba, and Seigo Yamauchi***

Institute for Chemical Reaction Science, Tohoku University, Katahira 2-1-1, Sendai 980-8577

†Department of Chemistry, Graduate School of Science, Tohoku University, Aramaki, Sendai 980-8578

(Received October 2, 1998)

Electron spin polarizations were studied for a system of excited triplet ($T_1$) phthalocyanine (MTNPc; M = $H_2$, Zn) and a nitroxide radical (TEMPO) in toluene solution by means of time-resolved EPR (TREPR) spectroscopy. TREPR spectra of the $T_1$ state and the radical (R) were observed simultaneously. Spin polarizations of both signals were found to consist of two components with different decay rates. From analyses of the polarizations and the decay curves, it was found that the triplet polarizations are generated from anisotropic $S_1 \rightarrow T_1$ intersystem crossings and thermal populations. The initial and late polarizations on TEMPO were interpreted in terms of electron spin polarization transfer (ESPT) from $T_1$ and a radical-triplet pair mechanism (RTPM) with a quartet precursor under $J < 0$ ($J$; exchange coupling parameter), respectively. The ESPT rate was determined and found to be dependent on temperature and the central atom(s) of MTNPc. In the $H_2$TNPc system, the ESPT rate is much slower than the diffusion rate and axial ligation of TEMPO remarkably accelerates the ESPT rate in the ZnTNPc system.

During the last two decades, time-resolved electron paramagnetic resonance (TREPR) spectroscopy has been found to be a very effective technique for studies of transient paramagnetic species in photochemical and photophysical processes.[1] Reaction intermediate radicals exhibit spin polarizations generated via radical–radical (R–R) interactions; this process is known as chemically induced dynamic electron polarization (CIDEP). The polarizations are interpreted in terms of two major mechanisms, the triplet mechanism (TM)[2] and the radical pair mechanism (RPM),[3] which are established both theoretically and experimentally.

In recent years, much attention has been drawn to electron spin polarizations produced via radical-triplet interactions.[4—9] The mechanisms have been studied in various radical (R) and triplet (T) systems and proposed as either the radical-triplet pair mechanism (RTPM)[4,5] or the electron spin polarization transfer (ESPT)[6,7] mechanism. The spin polarization due to RTPM has been reported rather extensively and is known to be generated from electron spin dipolar, Zeeman, and hyperfine couplings between quartet and doublet states, which are formed by an electron spin exchange interaction ($H_{ex} = -2JS_R \cdot S_T$) between R and T. The RTPM provides two kinds of polarizations such as A+A/E and E+E/A for doublet and quartet precursors, respectively, under $J < 0$; here A denotes an absorption and E an emission of a microwave.

On the other hand, for the ESPT a triplet polarization generated from a sublevel selective intersystem crossing is transferred to a radical through an exchange interaction; this process is similar to the TM in the R–R system. Although some observations had been likely to be interpreted by the ESPT,[7] no conclusive results were reported so far. The first definitive assignment of the ESPT has been given for a triplet porphyrin–nitroxide radical system by the help of direct observation of the transient EPR signal of the excited triplet ($T_1$) in solution.[6]

We have recently succeeded in observing the TREPR signals of $T_1$ phthalocyanines in solution. We present another insight into ESPT in this paper on the basis of analyses of spectra and decay curves of both $T_1$ and radical signals. Tetrakis(neopentyloxy)phthalocyanine (MTNPc; M = $H_2$, Zn) is selected as a $T_1$ molecule and 2, 2, 6, 6-tetramethyl-1-piperidinyloxyl (TEMPO) as a radical, as shown in Fig. 1. The induced spin polarizations are compared between the $H_2$TNPc and ZnTNPc systems, where the triplet polariza-

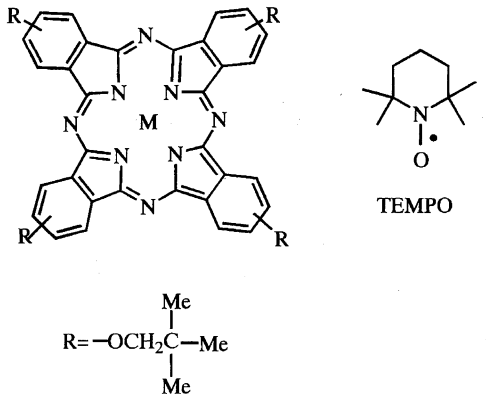


Fig. 1. Molecular structures of phthalocyanines examined and TEMPO.

tions are different depending on the central atom(s).[10] We obtain the ESPT rates, compare those between the two systems and with the diffusion rate, and discuss the results in terms of axial ligation and an exchange coupling between R and T.

## Experimental

$H_2$TNPc and ZnTNPc were synthesized according to the methods described in the literature.[11] TEMPO (Wako Pure Chemicals) and pyridine (Nacalai Tesque. Inc.) were used as received. Spectral grade toluene (Wako Pure Chemicals) was used as solvent without further purification. The typical concentrations of MTNPc and TEMPO were $2\times10^{-4}$ and $2\times10^{-3}$ M, respectively (1 M = 1 mol $dm^{-3}$). The solutions were deaerated by repeated freeze-pump thaw cycles using a vacuum line.

TREPR and steady state EPR measurements were carried out at various temperatures using a modified X-band JEOL JES FE2XG EPR spectrometer. Temperature was controlled by using a JEOL ES-DVT3 liquid $N_2$ flow system. TREPR signals from a modified EPR unit were integrated by a NF BX-531 boxcar integrator for spectra and by an Iwatsu DM 7200 digital memory for time-profiles. Time-resolution of our system is ca. 80 ns. The details of the TREPR apparatus have been described elsewhere.[12] An OPO laser (Spectra Physics, MOPO-710) pumped by a Nd : YAG laser (Spectra Physics GCR-170) was employed to excite selectively $H_2$TNPc and ZnTNPc to the $S_1$ states at 650 and 660 nm, respectively. The $g$ values were corrected with that of $^3C_{60}$ ($g$ = 2.0012).[13] T–T absorption measurements were performed by using a Nikon G250 monochromator and a Hamamatsu Photonics R928 photomultiplier with a cw Xe lamp (Hamamatsu C4263). The transient absorption experiment was made under the same conditions as that of the TREPR measurement, where the concentration of molecular oxygen is the same for both samples.

## Results and Discussion

We first describe a system of the $T_1$ state of MTNPc and then proceed to analyze polarizations of a radical and the triplet in the MTNPc–TEMPO system.

**1. $T_1$ Phthalocyanine.** TREPR spectra with a gate-time of 0.0—0.2 μs after the laser pulse were observed for $H_2$TNPc and ZnTNPc in toluene solution at room temperature (291 K), as shown in Figs. 2a and 2b, respectively. In each spectrum a single broad peak was observed with a full width at half maximum (fwhm) of ca. 10 mT. Spin polarizations of the signals are an emission (E) for $H_2$TNPc and an absorption (A) for ZnTNPc. In solid, well-known triplet spectra[10] were observed, as shown in Figs. 2c and 2d together with the spectral simulations.[14] The polarization patterns are EEE/AAA for $H_2$TNPc and AAA/EEE for ZnTNPc,[13] indicating that $T_1$ $H_2$TNPc and $T_1$ ZnTNPc provide totally emissive and absorptive polarizations, respectively, which are consistent with those observed in solution. All these results are similar to those observed for $T_1$ porphyrins[15] both in solution and solid. On the basis of these results, the observed signals in solution are reasonably assigned as the $T_1$ signals.

Time-profiles of the EPR signals in the two systems were obtained at room temperature (291 K) as shown in Figs. 3a and 3b. The signal of $T_1$ $H_2$TNPc shows two different polarizations, E and A, at earlier and later times, respectively. In

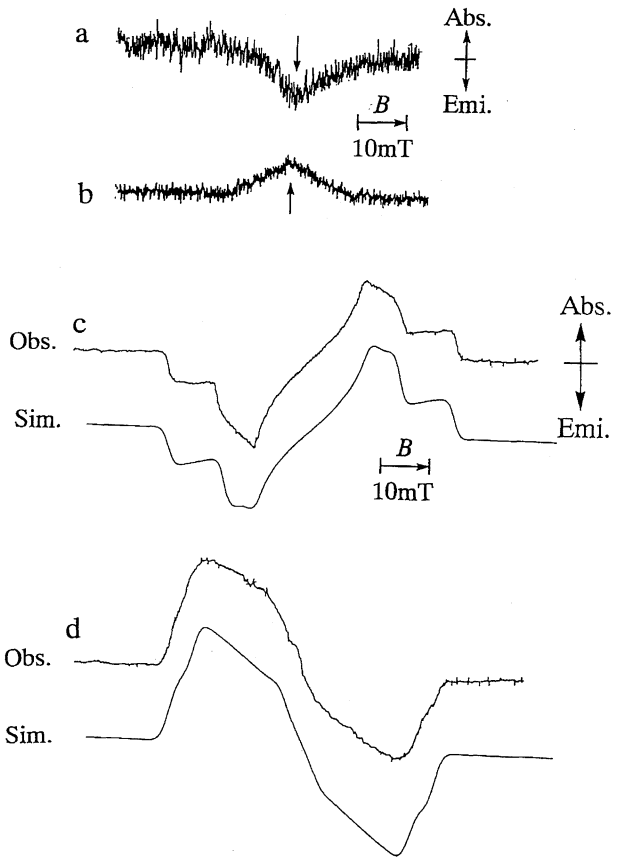


Fig. 2. TREPR spectra observed in toluene for (a) $H_2$TNPc and (b) ZnTNPc with a gate time 0.0—0.2 μs at 291 K and for (c) $H_2$TNPc and (d) ZnTNPc at 0.6—0.8 μs and 30 K together with the simulation. See Ref. 14 for the parameters used. Arrows indicate the fields where the time-profiles are observed (Fig. 3).

the case of $T_1$ ZnTNPc, the decay curve shows two absorptive components with faster and slower decays. The polarization of the fast component is an emission for $T_1$ $H_2$TNPc and an absorption for $T_1$ ZnTNPc, respectively in solution, which are the same as those observed in solid. In contrast, the slow components always show absorptive polarizations. From the polarization and the decay, one can conclude that the fast and slow components correspond to spin polarized ($^3$MTNPc$^\#$) and thermalized ($^3$MTNPc) triplets of MTNPc, respectively. Then the decay curves of the EPR signals $I_T$ are analyzed by a double exponential function as given by Eq. 1.[6b,13]

$$I_T([^3\text{MTNPc}^\#],[^3\text{MTNPc}])=A_1\exp\{-(k_T+k_d)t\}+A_2\exp\{-(k_d)t\}. \quad (1)$$

$A_1$ and $A_2$ are constants. $k_T$ and $k_d$ denote rates of spin lattice relaxation (SLR) and intrinsic decay in the $T_1$ state, respectively. The decay rate constants of $k_T$ and $k_d$ were obtained as 5.2 ($\pm$0.6)$\times10^6$ and 1.5 ($\pm$0.2)$\times10^4$ $s^{-1}$ for $H_2$TNPc and $>1\times10^7$ and 5.0 ($\pm$0.2)$\times10^4$ $s^{-1}$ for ZnTNPc. The decay rate of $^3$MTNPc is also obtained from an experiment of T–T absorption. Time-profiles were measured for $T_1$ $H_2$TNPc at 480 nm and for $T_1$ ZnTNPc at 490 nm, as shown in Fig. 4,

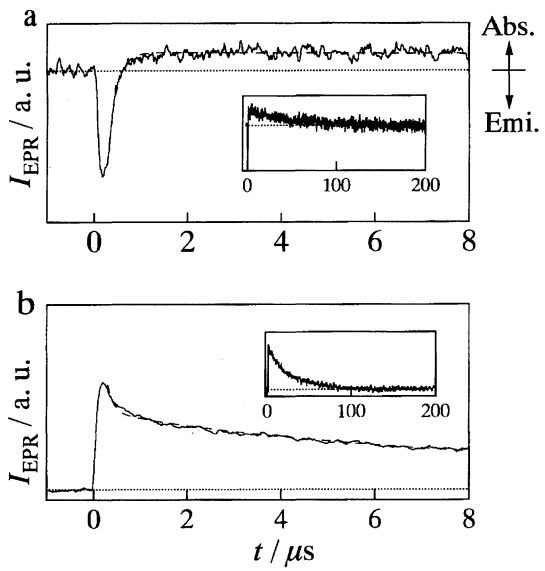


Fig. 3. Decay time-profiles of EPR signals of (a) $H_2$TNPc and (b) ZnTNPc at 291 K in toluene. The inserts show the decays with the different time scale. The simulation curves (dashed lines) are also shown.

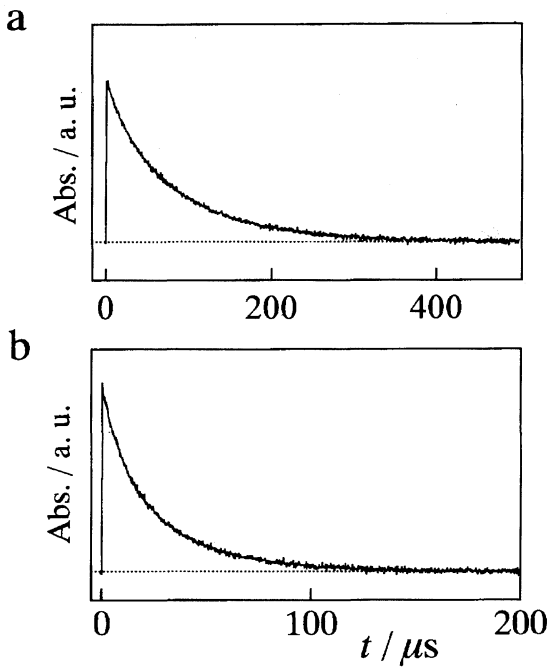


Fig. 4. Decay profiles of T–T absorptions of (a) $H_2$TNPc and (b) ZnTNPc in toluene solution at 291 K. The simulation curves are shown by dashed lines.

and were analyzed by a single exponential function. The obtained decay rate constants are 1.4 ($\pm$0.1)$\times 10^4$ for $H_2$TNPc and 5.0 ($\pm$0.2)$\times 10^4$ $s^{-1}$ for ZnTNPc, which agree well with those of the slow component of the EPR signal in both systems. The decay curves of the EPR signals were measured at different temperatures and analyzed similarly. The obtained values are summarized in Table 1.

It is found that the SLR rate decreases with temperature and is faster for $T_1$ ZnTNPc than for $T_1$ $H_2$TNPc. These results are qualitatively consistent with those of $T_1$ porphyrins and are interpreted in terms of two relaxation mechanisms involving fluctuations of dipole–dipole and spin-rotation interactions,[15] respectively.

**2. Electron Spin Polarization Transfer. 2.1 Existence of ESPT.** TREPR spectra were obtained for $H_2$TNPc–TEMPO in toluene at 291 K, as shown in Figs. 5a, 5b, and 5c. In the spectrum at 0.1—0.3 μs, there are two kinds of emissive signals: one broad peak with fwhm of ca. 10 mT and three relatively sharp peaks with EPR parameters of $g = 2.0061\pm0.0002$ and $A_N = 1.55\pm0.02$ mT. The former is easily assigned to that of polarized $T_1$ $H_2$TNPc in comparison with the $T_1$ spectrum assigned in a previous section (Fig. 2a). For the latter, the signal is assigned as that of the TEMPO radical from the reported EPR parameters ($g = 2.006$, $A_N = 1.55$ mT).[6] The spin polarizations of the TEMPO signal observed at 0.2—0.4 μs and 3.0—3.2 μs (Figs. 5b and 5c) were both emissive in this system. TREPR spectra were also observed for the ZnTNPc–TEMPO system, as shown in Figs. 5d and 5e, where two different polarizations on the TEMPO signal were observed as A at earlier times and E at later times. These polarizations together with the $T_1$ polarization are summarized in Table 2. It is found that the TEMPO polarization at earlier times is different between the two systems, but is the same as the polarization of the corresponding $T_1$ state. In contrast, the polarizations are emissive at later times in both systems.

Time-profiles of the $T_1$ and radical signals are shown in Figs. 6a and 6b for the $H_2$TNPc–TEMPO system and in Figs. 6c and 6d for the ZnTNPc–TEMPO system at 291 K.

Table 1. Various Decay Rate Constant[a]

| | MTNPc | | MTNPc–TEMPO | | |
|---|---|---|---|---|---|
| | $T_1$ signal | | ($T_1$, TEMPO) signals | | |
| System/Temp | $k_T/10^6$ $s^{-1}$ | $k_d/10^4$ $s^{-1}$ | $k'_T/10^6$ $s^{-1}$ | $k_d/10^4$ $s^{-1}$ | $k_R/10^6$ $s^{-1}$ |
| $H_2$TNPc/291 K | 5.2 | 1.5 (1.4)[b] | 7.7 | 2.4 (2.3) | 2.5 |
| /243 K | 1.9 | 1.1 | 2.7 | 1.9 | 2.0 |
| /213 K | 1.5 | 0.65 | 2.1 | 1.3 | 1.3 |
| ZnTNPc/291 K | >10 | 5.0 (4.5) | — | 16.7 (16.7) | 2.6 |
| /213 K | 4.9 | 1.2 | 6.7 | 3.3 | 1.4 |

a) For an error of each value, see the text. b) Numbers in parentheses indicate the $T_1$ decay rate constants obtained from the T–T absorption experiment.

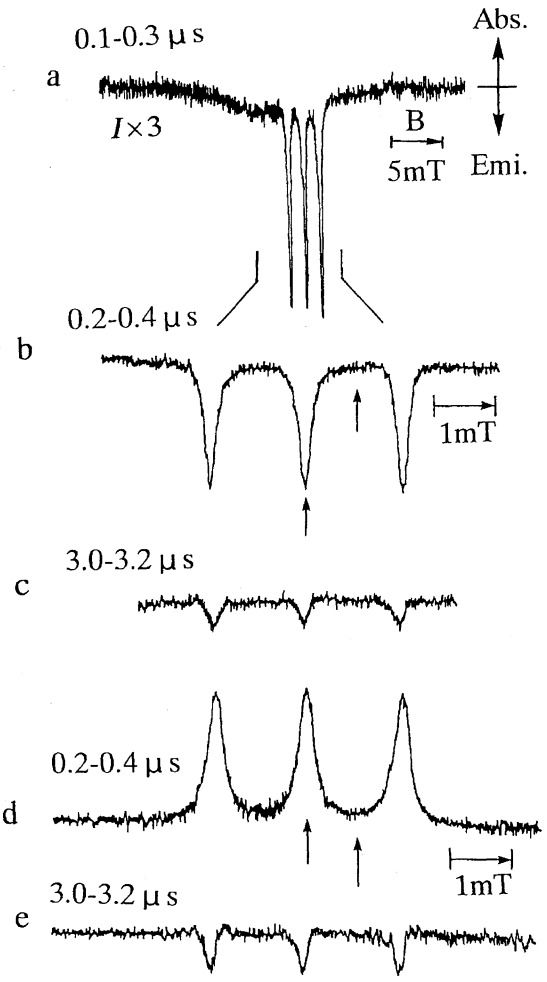


Fig. 5. TREPR spectra observed at various gate times for the $H_2$TNPc (a, b, c)- and ZnTNPc (d, e)–TEMPO systems at 291 K in toluene. Arrows indicate the fields where the time-profiles are observed (Fig. 6).

Table 2. Spin Polarizations Observed for $T_1$ Phthalocyanine and TEMPO[a)]

| | $T_1$ MTNPc | TEMPO–MTNPc | |
|---|---|---|---|
| System | | Fast | Slow |
| $H_2$TNPc | E | E | E |
| ZnTNPc | A | A | E |

a) E and A denote an emission and an absorption of microwave, respectively.

The time-profiles were also observed at different temperatures; those at 213 K are shown in Fig. 7. As for the TEMPO signal, two kinds of polarizations of fast and slow components were observed, consistent with the TREPR spectra (Fig. 5). The fast component of the TEMPO signal shows the same polarization as $T_1$ MTNPc, emissive for the $H_2$TNPc system and absorptive for the ZnTNPc system, which is consistent with the ESPT occurring from $T_1$MTNPc to TEMPO. The slow component shows an emission in the two systems regardless of the $T_1$ polarization. The E polarization is just the same as the RTPM polarization with quartet precursors

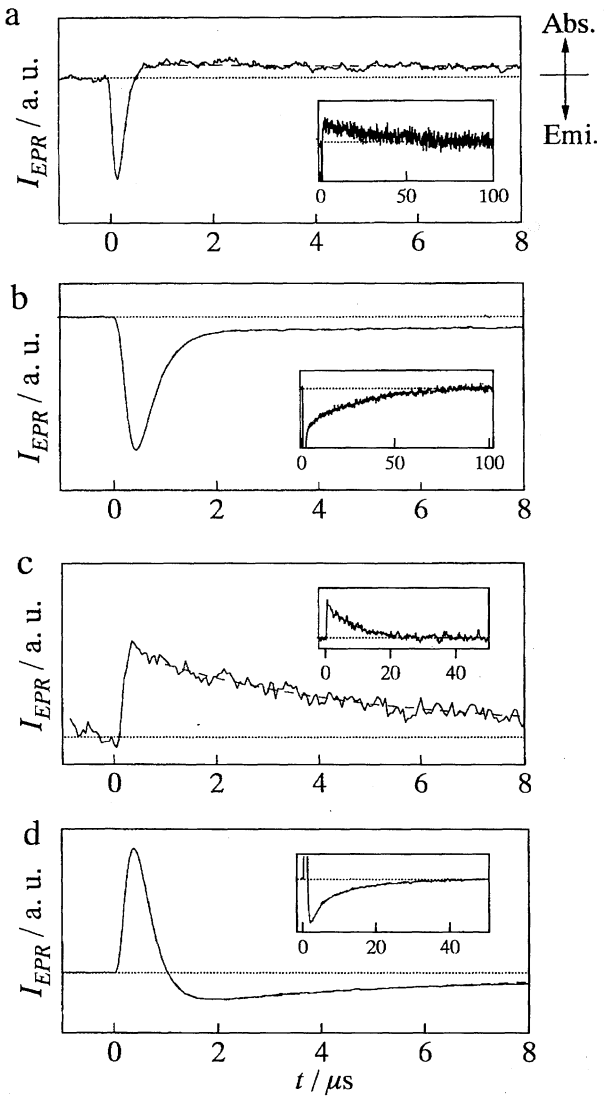


Fig. 6. Time-profiles of the EPR signals of (a) $T_1$ $H_2$TNPc and (b) TEMPO for the $H_2$TNPc–TEMPO system and those of (c) $T_1$ ZnTNPc and (d) TEMPO for the ZnTNPc–TEMPO system at 291 K together with the simulation curves.

under $J < 0$. On the basis of these considerations, we analyze the decay curves in terms of the ESPT and the RTPM.[6b)] Reaction and spin dynamics are expressed as follows:

a) ESPT

$$^3\text{MTNPc}^{\#} + \text{TEMPO} \rightarrow {}^3\text{MTNPc} + \text{TEMPO}^{\#} \quad : k_{\text{ESPT}} \qquad (2)$$

b) RTPM

$$(^3\text{MTNPc}^{\#}, {}^3\text{MTNPc}) + \text{TEMPO} \rightarrow \text{MTNPc} + \text{TEMPO}^{\#} \quad : k_{\text{q}} \qquad (3)$$

c) SLR

$$^3\text{MTNPc}^{\#} \rightarrow {}^3\text{MTNPc} \quad : k_{\text{T}} \qquad (4)$$

$$\text{TEMPO}^{\#} \rightarrow \text{TEMPO} \quad : k_{\text{R}} \qquad (5)$$

d) intrinsic decay

$$(^3\text{MTNPc}^{\#}, {}^3\text{MTNPc}) \rightarrow \text{MTNPc} \quad : k_{\text{d}} \qquad (6)$$

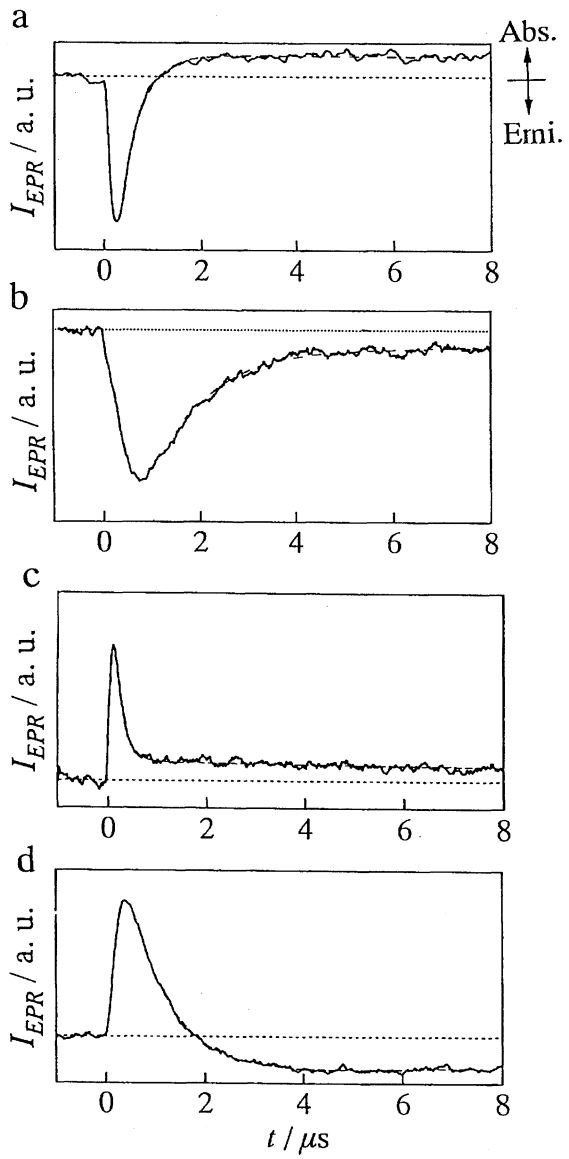


Fig. 7. Time-profiles of the EPR signals of (a) $T_1$ $H_2$TNPc and (b) TEMPO for the $H_2$TNPc–TEMPO system and (c) $T_1$ ZnTNPc and (d) TEMPO for the ZnTNPc–TEMPO system at 213 K.

Here we assume that the ESPT and RTPM are pseudo-first-order processes, because [$^3$MTNPc] ≪ [TEMPO]. The decay of a sum of polarized and thermalized $T_1$ MTNPc signals $I'_T$ is expressed with a double-exponential function as

$$I'_T([^3\text{MTNPc}^{\#}], [^3\text{MTNPc}]) = A_3 \exp\{-(k'_T)t\} + A_4 \exp\{-(k'_d)t\} = A_3 \exp\{-(k_T + k_d + k'_{ESPT} + k'_q)t\} + A_4 \exp\{-(k_d + k'_q)t\}. \quad (7)$$

$A_3$ and $A_4$ are constants. $k'_{ESPT}$ and $k'_q$ denote rate constants for processes of ESPT and quenching of $T_1$ with TEMPO including RTPM, respectively, as $k'_{ESPT} = k_{ESPT}$[TEMPO] and $k'_q = k_q$[TEMPO]. From the analysis using Eq. 7, $k'_T (= k_T + k_d + k'_{ESPT} + k'_q)$ and $k'_d (= k_d + k'_q)$ were obtained as 7.7 $(\pm 0.5) \times 10^6$ and 2.4 $(\pm 0.2) \times 10^4$ $s^{-1}$, respectively in the $H_2$TNPc system with [TEMPO] = 2 mM. By comparing these values with already given $k_T$ and $k_d$ values (Table 1), $k'_{ESPT}$ and $k'_q$ are obtained as $2.5 \times 10^6$ and $0.9 \times 10^4$ $s^{-1}$, respectively. The rate constants were also obtained at different temperatures and are summarized in Table 1. For the decay curve of $T_1$ ZnTNPc at 291 K (Fig. 6c), the first component is missing and the decay is analyzed by a single exponential function. This means that the rate of the ESPT process exceeds our time resolution (80 ns).

The overall (rise and decay) time-profile of the TEMPO signal should be analyzed by using the Bloch equation,[16] because the spin relaxation rates are comparable with those of the other processes. However, in our systems, as lineshapes of the TEMPO signal are not totally Lorentzian under [TEMPO] < 5 mM, the Bloch equation is not applicable for analysis. Then we only analyze the decay of the TEMPO signal by using kinetic equations. The following equation with a double exponential function is obtained for the decay of the TEMPO signal $I_R$.[6b,17]

$$I_R([\text{TEMPO}^{\#}]) = A_5 \exp\{(-k_R)t\} + A_6 \exp\{(-k'_d)t\} = A_5 \exp\{(-k_R)t\} + A_6 \exp\{-(k_d + k'_q)t\}. \quad (8)$$

$A_5$ and $A_6$ are constants. $k_R$ denotes a SLR rate of TEMPO. Equation 8 shows that the ESPT and RTPM polarizations decay with $k_R$ and $k'_d$, respectively under the condition $k_R > k'_d$. The decay curves were analyzed for the two systems; the obtained parameters are summarized in Table 1. The obtained $k_R$ values (2.6 and $2.5 \times 10^6$ $s^{-1}$) at 291 K are consistent with the reported SLR rate of TEMPO ($2.3 \times 10^6$ $s^{-1}$).[18] The decay constants of $T_1$ MTNPc $k'_d$ $(= k_d + k'_q)$ were obtained separately from the T–T absorption experiment and are in good agreement with the EPR data within experimental error (Table 1). These results support the validity of the decay analyses of the TEMPO signal on the basis of the two polarization mechanisms.

Therefore, we conclude that the polarization of the $T_1$ state is transferred to the TEMPO radical via the ESPT, competing with the SLR process in $T_1$. Another emissive polarization on TEMPO is generated via radical-triplet couplings, namely the RTPM.

**2.2. ESPT Rate Constant.** The ESPT rate $k_{ESPT}$ was determined from the decay analysis of the $T_1$ signals. We first check the assumption of the pseudo-first-order process for ESPT by changing the concentration of TEMPO. In order to measure the rate over a wide range of the concentration, we selected the system of $H_2$TNPc–TEMPO at 243 K in consideration of the SLR rate and the time resolution of the system. The decay of the polarized $T_1$ $H_2$TNPc signal was analyzed similarly to those in the previous section for systems with and without TEMPO. The plots of the ESPT rate vs. the concentration of TEMPO are shown in Fig. 8, where the rate increases linearly with [TEMPO]. From this result, the validity of the assumption is proved and the second-order rate constant of ESPT was obtained as 0.38 $(\pm 0.03) \times 10^9$ $M^{-1}$ $s^{-1}$ at 243 K. At other temperatures, we measured the rate $k'_{ESPT}$ at 2 mM TEMPO and calculated the second-order

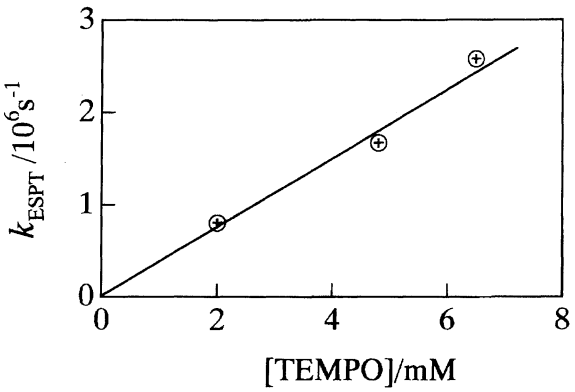


Fig. 8. Plots of the ESPT rate $k_{ESPT}$ vs. the TEMPO concentration for the $H_2$TNPc–TEMPO system at 243 K.

rate constant, as summarized in Table 3. It is found that the ESPT rate constant decreases with lowering temperature and that the rate is faster in the ZnTNPc system than in the $H_2$TNPc system.

Next we compare these values with the diffusion rate constant, which is calculated by using the Smoluchowski eqation[19] as,

$$k_{dif} = 4 \times 10^{-3} \pi (r_{Pc} + r_{TEMPO})(D_{Pc} + D_{TEMPO}) N_a \quad (9)$$

where $N_a$ denotes the Avogadro number, $r_{Pc}$ and $r_{TEMPO}$ are encounter cross-sections, and $D_{Pc}$ and $D_{TEMPO}$ are diffusion coefficients of MTNPc and TEMPO, respectively. The diffusion coefficients are calculated by the Stokes–Einstein relation,[20] using $r_{Pc}$ (6 Å),[11] $r_{TEMPO}$ (2 Å)[6] and viscosity of toluene $\eta_T$ (cP = mPa s)[21] at temperature $T$(K). The values are summarized in Table 3. In the $H_2$TNPc system, the obtained ESPT rate constants are much smaller than the calculated diffusion rate constants at all temperatures examined. In contrast, in the ZnTNPc–TEMPO system the ESPT rate is larger and on the same order of the diffusion rate. It was also reported that the ESPT occurs with the same order of the diffusion rate in the Zn porphyrin–TEMPO system.[6]

In order to clarify the reason for the difference in the ESPT rate between the two systems, we examined interactions between MTNPc and TEMPO by observing UV-vis absorption spectra. The spectra were observed with and without TEMPO, as shown in Fig. 9; no appreciable effect is found for the $H_2$TNPc–TEMPO system. In contrast, some specific interaction such as axial ligation is indicated from the spectrum (Fig. 9b) in the ZnTNPc–TEMPO system. This

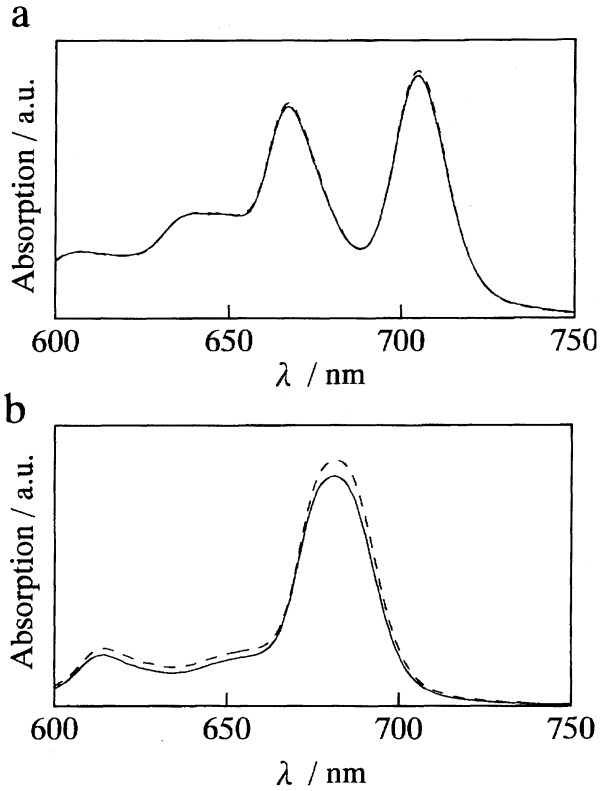


Fig. 9. Absorption spectra of (a) $H_2$TNPc (- - -) and that with 20 mM TEMPO (——) and (b) ZnTNPc (- - -) and that with 20 mM TEMPO (——) at 291 K in toluene. The absorption due to TEMPO was subtracted from the spectra.

consideration is confirmed by the TREPR experiment using pyridine. When 0.5 M pyridine is added to the system, all ZnTNPc's ligate with pyridine; this was found from the result of concentration dependence of the visible absorption spectra. Under 0.5 M pyridine, the decay of the triplet signal was analyzed with and without TEMPO at 213 K. The ESPT rate constant was obtained as $0.30 \times 10^9$ $M^{-1}$ $s^{-1}$, which is much smaller than that ($1.0 \times 10^9$ $M^{-1}$ $s^{-1}$) obtained for the system without pyridine. The value is similar to that ($0.30 \times 10^9$ $M^{-1}$ $s^{-1}$) in the $H_2$TNPc system (Table 3). On the basis of these results, we interpret that the larger ESPT rate is due to axial ligation of TEMPO to $T_1$ ZnTNPc, which causes the larger spin exchange interaction ($J$) and more efficient ESPT in the ZnTNPc system.

In these systems we also obtained the rate $k_q$ (Table 3)

Table 3. ESPT and Quenching Rate Constants and Calculated Diffusion Rate Constants

| System/Temp | $k_{ESPT}/M^{-1} s^{-1}$ $10^9$ | $k_q/M^{-1} s^{-1}$ $10^7$ | $k_{dif}/M^{-1} s^{-1}$ $10^9$ |
|---|---|---|---|
| $H_2$TNPc/291 K | 1.3 | 0.45 | 15 |
| /243 K | 0.38 | 0.41 | 4.4 |
| /213 K | 0.30 | 0.32 | 1.9 |
| $H_2$TNPc-Py/213 K | 0.39 | 0.26 | 1.9 |
| ZnTNPc/291 K | — | 5.9 | 15 |
| /213 K | 1.0 | 1.1 | 1.9 |
| ZnTNPc-Py/213 K | 0.30 | 0.77 | 1.9 |

of the triplet quenching, which includes the RTPM process. The quenching process is much slower, at least by two orders of magnitudes, than the ESPT process. This might be due to the fact that the lowest excited doublet ($D_1$) state (ca. 18000 $cm^{-1}$) of TEMPO locates higher than $T_1$ MTNPc (14000—16000 $cm^{-1}$) in energy,[6] where no energy transfer occurs from $T_1$ to $D_1$.[8]

## Conclusion

We have investigated electron spin polarizations generated via interactions between excited triplet ($T_1$) phthalocyanines and the TEMPO radical in toluene solution by time-resolved EPR. Direct observations of the EPR signals of $T_1$ and the radical provided definitive evidence for the electron spin polarization transfer (ESPT) occurring in fluid solution. This is the second example of ESPT proved experimentally. From the decay analyses, it was found that the ESPT rate is not diffusion-controlled in the $H_2$TNPc system and increases with axial ligation in the ZnTNPc system. The other polarization mechanism of the radical-triplet pair mechanism (RTPM) was also found to be involved in these systems.

This work was supported by Research Fellowships of the Japan Society for the Promotion of Science for Young Scientists (JF) and a Grant-in-Aid for Scientific Research No. 08554025 from the Ministry of Education, Science, Sports and Culture.

## References

1) A. J. Hoff, "Advanced EPR," Elsevier, Amsterdam (1989), Chap. 10, and references therein.

2) a) S. K. Wong, D. A. Hutchison, and J. K. S. Wan, *J. Chem. Phys.*, **59**, 985 (1973); b) P. W. Atkins and G. T. Evans, *Mol. Phys.*, **27**, 1633 (1974).

3) a) F. J. Adrian, *J. Chem. Phys.*, **54**, 3918 (1971); b) F. J. Adrian and L. Monchick, *J. Chem. Phys.*, **71**, 2600 (1979).

4) C. Blättler, F. Jent, and H. Paul, *Chem. Phys. Lett.*, **166**, 375 (1990).

5) a) A. Kawai, T. Okutsu, and K. Obi, *J. Phys. Chem.*, **95**, 9130 (1991); b) A. Kawai and K. Obi, *J. Phys. Chem.*, **96**, 52 (1992); *Res. Chem. Intermed.*, **19**, 865 (1993).

6) a) J. Fujisawa, K. Ishii, Y. Ohba, M. Iwaizumi, and S. Yamauchi, *J. Phys. Chem.*, **99**, 17082 (1995); b) J. Fujisawa, Y. Ohba, and S. Yamauchi, *J. Phys. Chem. A*, **101**, 434 (1997).

7) T. Imamura, O. Onitsuka, and K. Obi, *J. Phys. Chem.*, **90**, 6741 (1986).

8) W. S. Jenks and N. J. Turro, *J. Chem. Intermed.*, **13**, 237 (1990).

9) J. Fujisawa, K. Ishii, Y. Ohba, S. Yamauchi, M. Fuhs, and K. Möbius, *J. Phys. Chem. A*, **101**, 5869 (1997).

10) a) K. Akiyama, S. T. Kubota, and Y. Ikegami, *Chem. Phys. Lett.*, **185**, 65 (1991); b) R. Miyamoto, S. Yamauchi, N. Kobayashi, T. Osa, Y. Ohba, and M. Iwaizumi, *Coord. Chem. Rev.*, **137**, 57 (1994).

11) N. Kobayashi, H. Lam, W. A. Nevin, P. Janda, C. C. Leznoff, T. Koyama, A. Monden, and H. Shirai, *J. Am. Chem. Soc.*, **116**, 897 (1994).

12) S. Ohkoshi, S. Yamauchi, Y. Ohba, and M. Iwaizumi, *Chem. Phys. Lett.*, **244**, 313 (1994).

13) J. Fujisawa, Y. Ohba, and S. Yamauchi, *Chem. Phys. Lett.*, **282**, 181 (1997).

14) The observed TREPR spectra of $T_1$ $H_2$TNPc and $T_1$ ZnTNPc in toluene glass at 30 K were simulated with the zero-field splittings (zfs') and the intersystem crossing ratio of $D = 0.77$ GHz, $|E| = 0.055$ GHz and $P_x : P_y : P_z = 0.55 : 0.45 : 0$ and $D = 0.72$ GHz, $|E| = 0.16$ GHz and $P_x : P_y : P_z = 0 : 0.25 : 0.75$, respectively. The z principal axis of the zfs is perpendicular to the phthalocyanine plane.

15) J. Fujisawa, Y. Ohba, and S. Yamauchi, *J. Am. Chem. Soc.*, **119**, 8736 (1997).

16) N. C. Verma and R. W. Fessenden, *J. Chem. Phys.*, **65**, 2139 (1976).

17) K. Ohara and N. Hirota, *Bull. Chem. Soc. Jpn.*, **69**, 1517 (1996).

18) a) R. N. Schwartz, L. L. Jones, and M. K. Brown, *J. Phys. Chem.*, **83**, 3429 (1979); b) I. V. Koptyug, S. H. Bossmann, and N. J. Turro, *J. Am. Chem. Soc.*, **118**, 1435 (1996).

19) M. Smoluchowski, *Z. Phys. Chem.*, **92**, 129 (1917).

20) A. D. Osborne and G. Porter, *Proc. R. Soc. London, Ser. A*, **A284**, 6 (1965).

21) H. van Willigen and K. P. Dinse, *J. Phys. Chem.*, **98**, 7464 (1994).